ANALYSIS OF STRUCTURAL, VIBRATIONAL (FTIR AND FT RAMAN) AND ELECTRONIC (UV-VIS) PROPERTIES OF ACETAZOLAMIDE USING DFT METHOD

- D. Bakkiyaraj[a]*

- S. Periandy[b]

- K. Carthigayan[a]

- S. Xavier [ac]

ABSTRACT

The structural analysis of Acetazolamide molecule has been carried out using DFT computational method with the functional B3LYP/ 6-311++ G (d, p). The computed values are compared with the XRD data and deviations are discussed. The fundamental modes of vibrations of the molecule were assigned with the help of the data obtained from TED using VEDA program. The assignments were compared with wavenumbers of the FTIR and FT-Raman spectra. The ranges of the values are observed to be closer to the experimental values. The Chemical shifts 13C and proton were computed using GIAO method with the help of potential continuum modal, and the values are closer to the experimental values. Along with these, the electronic transitions of the molecule were computed from the UV-Vis analysis and possible charge transfer is calculated from the HOMO-LUMO representation pictures. The Lewis and non-Lewis orbital analysis revealed knowledge of the charge delocalization in the molecule from the NBO discussion. By MEP investigation the electron cloud map exhibited the positive and negative charge delocalization in the molecule. Through the NLO studies the molecule is found to be a candidate for the NLO material. The temperature dependence of different thermodynamical properties was also investigated. The spectroscopic results are correlated with the data obtained from the quantum computational methods. And the results are discussed.

Keywords: Acetazolamide, Chemical shift, NBO, HOMO-LUMO, FT-IR.

INTRODUCTION

Acetazolamide is known as 1,3,4-thiadiazole-2-sulfonamide-5-acetamido. The chemical formula is $C_4H_6N_4O_3S_2$. Sulfonamides are one of the well-known inhibitors of carbonic anhydrase with acetazolamide [1]. Clinically this is used for the treatment of glaucoma and it is prescribed as a drug to decrease the intraocular pressure in a human eyes. They are most powerful agent to lower the intraocular pressure [2]. However, due to extraocular side effects, it has become less popularized. It is also used for treating high altitude

[a]Research Scholar, R & D, Bharathiyar University, Coimbatore, Tamil Nadu, India.

[b]Department of Physics, Kanchi Mamunivar Centre for Post Graduate Studies, Puducherry, India.

[c]Department of Physics, St. Joseph College of Arts and Science, Cuddalore, Tamil Nadu, India.

*Corresponding author E-mail address: bakkiyaraj2009@gmail.com, Tel: +91 9994260309.

sickness like epilepsy and prophylaxis [2-4]. Recently it has been used against the side effects of drugs in influenza and respiratory diseases [5, 6]. Carbonic anhydrase inhibitor derivatives of acetazolamide, whose derivative were proved for the growth of several tumor cells lines in vitro and vivo [7]. The crystal structure of acetazolamide has been discussed by Mathew et al [1]. It was found that the acetazolamide has triclinic structure with space group P1. Baraldi et al. [8] have made a polymorphism study on acetazolamide using FTIR/ATR and DSC (Differential scanning calorimetry) measurements. I.P. Kaur et al. [2] have made a review study on acetazolamide and its glaucoma therapeutic uses. It has been reported that the acetazolamide is more physiologically effective than 2% of dorzolamide hydrochloride. S. Chakravarty et al. [3] made a crystallographic study on this molecule and found the active sites of enzyme and orientation of sulfonamide inter and intra molecular hydrogen bonds and its interactions with sulfonamide.

Lot of works have been reported on acetazolamide [1-25] based on its applications. However, HOMO-LUMO, Non linear optical (NLO) property, NMR and thermodynamic studies supported by quantum computations have not been reported so far on acetazolamide inspite of its varied biological applications. Hence, a detailed conformational analysis with quantum computational study of HOMO-LUMO, vibrational modes and optical - electronic properties of the molecule is carried out in the present work. To know the reactivity center and the chemical shift of carbon and hydrogen atoms in the molecule, the atomic charge analysis by Mullikan population analysis (MPA) and atomic polar tensor (APT) charge analysis were also carried out.

EXPERIMENTAL DETAILS

The compound acetazolamide of spectroscopic grade is purchased from Sigma–Aldrich Chemicals, USA. ABB-MB3000 spectrometer was used to record FT-IR spectrum of the compound in the range of 4000–400 cm^{-1}, it resulted with the scanning speed of 30 cm^{-1} min^{-1} and spectral width 2 cm^{-1}. The frequencies of all sharp bands are accurate to ±1 cm^{-1}. Hariba-Jobin, Lab RAM HR- Raman Spectrometer was used for recording FT-Raman spectrum of the compound in the range of 4000-10 cm^{-1} with the He-Ne (632nm) laser source. For recording 1H and 13C NMR spectra in DMSO solvent, high resolution 300 MHz and 75 MHz NMR spectrometer were used respectively. The UV spectra is recorded dissolved in ethanol solvent and recorded between the wavelength range of 200 nm to 400 nm with the scanning interval of 0.2nm and slit width 1.0 nm using the UV-1700 series instrument.

COMPUTATIONAL DETAILS

The entire calculations were performed using density functional theory (DFT) with B3LYP and B3PW91 functional and basis set 6-311++ G (d, p) on a personal computer using GAUSSIAN 09W program package [26, 27]. The geometry of the title molecule acetazolamide is fully optimized by Berny's optimization algorithm using redundant internal co-ordinates. To rationalize the experimental and computed values a scale factor is applied and the vibrational frequencies are scaled down with scaling factor 0.9850 for B3LYP and 0.9750 for B3PW91method. All the normal modes of the vibrations are assigned based on the total energy distribution (TED) values computed using vibrational energy distribution analysis (VEDA 4) program [28- 31], and also in comparison with the literatures and Gauss view programs [27].The geometry of the title molecule acetazolamide is fully optimized using B3LYP functional with 6-311++G (d, p) basis set and the same geometry is used for the conformational analysis using semi-empirical method parameterization (PM6). The natural bonding orbital (NBO) and HOMO-LUMO were also calculated using same method and basis set. The UV-Vis electronic transitions are predicted with time dependent self consistent field (TD-SCF) method in combination with B3LYP/6-311++ G (d, p) and the solvent effect is introduced by integral equation formalism-polarizable continuum model (IEF-PCM) method [32,33]. Similarly the NMR chemical shifts are also carried out by gauge invariant atomic orbital (GIAO) [34] method in combination with B3LYP/6-311G + (2d, p) in gas phase, along with IEF-PCM method to study the impact of solvent effect.

RESULTS AND DISCUSSION

Geometrical Analysis

The optimized molecular structure of the molecule acetazolamide along with the numbering of atoms is shown in Fig. 1. The optimized structure parameters of acetazolamide calculated by B3LYP and B3PW91 functional with the basis set 6-311++G (d, p) are listed in Table 1 and values are compared with the crystallographic data. The C-C bond length within benzene ring is generally lie in the range 1.38-1.40 Å because of the conjugation effect, in the present molecule there is no such C-C bond, there is only one C14-C15 bond in acetamido part of the molecule with length 1.510 Å in B3LYP and 1.504 Å in B3PW91 method, which is slightly higher than the experimental value 1.48 Å. This is C-C single bond length value, which shows that the C-C bond present in this molecule is a purely single bond which does not undergo any conjugational effect.

single bonded [35] and the optimization has brought slight constriction on these bond lengths. There are three C-S bonds in the molecule, all of them are single bonded but two of them are within the thia diazole ring and the third one is outside the ring. The values found for bonds within the ring is 1.745 Å and for out side the ring is 1.799 Å, which shows that the bond lengths are shortened in ring formation whereas it remains unaffected outside. The experimental and theoretical values of C14=O18 are 1.219 Å and 1.215 Å in B3LYP 1.213 Å in B3PW91 respectively. This shows that C=O bond length does not undergo any change and remain unaffected in this molecule.

The bond angle analysis shows that the computed S3-C1=N4 bond angle is 115.55^0 in B3LYP and 115.60^0 in B3PW91. Similarly, the bond angle at S3-C2=N5 is 115.83^0 in B3LYP and 115.83^0 in B3PW91. The experimental value in both the case is 115^0, this shows that the thiadiazole ring is highly symmetrical about the carbon atoms and remains unaffected by the substitutions on both sides. The bond angles around

Fig. 1: Optimized Structure of Acetazolamide

For C-H bonds, there are three such bonds; all of them have the value 1.091 Å which is exactly in agreement with the experimental value 1.090 Å. This shows there is no influence on these bonds in this molecule. An interesting observation has been noted in the case of CN bonds; There are two C=N and two C-N in the molecule, which is confirmed by the bond length values. C1=N4 has bond length value 1.309 Å, where as C2=N5 has value 1.290 Å, this shows both are double bonded but there is slight difference between them, which is obviously due to the two different atoms S and N with which these carbon atoms C1 and C2 atoms are bonded. The other two bonds C14-N6 and C1-N6 both have bond length values around 1.38 Å which differs with the experimental value 1.369 and 1.333 Å. This observation shows that both of them are

the N atoms in the ring shows that the bond angle at C1=N4-N5 is 111.95^0 in B3LYP and 111.89^0 in B3PW91 but the experimental angle 112.7^0, whereas the angle at C2=N5-N4 is 112.49^0 in B3LYP and 112.43^0 in B3PW91 with its experimental value 112.53^0. This shows that there is a small asymmetry in the angles around the N atoms in the thiadiazole ring which may be due the difference in the substitution on both sides of the ring. The angle at one side of the ring N5=C2-S7 is 122.43^0 in B3LYP and 122.52^0 in B3PW91 and the experimental value is 120.4^0; the angle at the other side N4=C1-N6 is 120.10^0 in B3LYP and 120.16^0 in B3PW91 and the experimental value is 119.6^0.

Similarly the bond angle at N6-C14=O18 is 120.89^0 in B3LYP and 120.79^0 in B3PW91 but the experimental value is 119.9^0; this is the typical bond angle generally

formed inside the benzene ring at any carbon atoms. The experimental deviation is may be due to the influence of the hybridization of N and O atoms around this carbon atom. The angles at the methyl group in this molecule are found to be unaffected. One notable observation in the bond angles of the present molecule is difference between the experimental and computed values. There is a good agreement between the values computed by the two methods B3LYP and B3PW91, but there is a significant difference between the experimental and computed values for most of the bond angles, which may be due to the presence of highly electronegative atoms like O and N in the present molecule.

Table 1: The Optimized Geometrical parameters of Acetazolamide

Geometrical parameter	B3LYP/ 6-311++G (d, p)	B3PW91/ 6-311++G (d, p)	XRD[a]
Bond length(A⁰)			
C14-C15	1.510	1.504	1.480
C15-H16	1.091	1.091	1.090
C15-H17	1.091	1.091	1.090
C15-H19	1.092	1.092	1.090
C1=N4	1.309	1.309	1.369
C1-N6	1.379	1.375	1.333
C2=N5	1.290	1.290	1.283
C14-N6	1.385	1.381	1.369
C14=O18	1.215	1.213	1.322
N4-N5	1.360	1.351	1.374
N6-H13	1.011	1.010	0.837
C1-S3	1.745	1.734	1.737
C2-S3	1.753	1.742	1.728
C2-S7	1.799	1.788	1.767
N10-H11	1.014	1.013	0.820
N10-H12	1.014	1.013	0.820
N10-S7	1.677	1.665	1.594
S7=O8	1.451	1.446	1.427
S7=O9	1.458	1.453	1.432
Bond Angle(⁰)			
S3-C1=N4	115.55	115.60	115.3
S3-C1-N6	124.33	124.23	125.1
N4=C1-N6	120.10	120.16	119.6
S3-C2=N5	115.83	115.83	116.4
S3-C2-S7	121.71	121.62	120.4
N5=C2-S7	122.43	122.52	120.4
C1-S3-C2	84.14	84.23	85.0
C1=N4-N5	111.95	111.89	112.08
C2=N5-N4	112.49	112.43	112.53
C1-N6-H13	114.49	114.61	115.0
C1-N6- C14	124.90	124.54	124.7
H13-N6-C14	120.60	120.83	120
C2-S7=O8	108.00	107.92	106.6
C2-S7=O9	105.28	105.24	105.4
C2-S7-N10	102.37	102.46	106.6
O8=S7=O9	122.98	123.03	121.2
O8=S7-N10	109.42	109.40	108.4
O9=S7-N10	106.82	106.84	107.8
S7-N10-H11	111.91	112.13	106
S7-N10-H12	110.80	111.04	106
H11-N10-H12	113.28	113.51	
N6-C14-C15	115.61	115.64	114.6
N6-C14=O18	120.89	120.79	120.9
C15-C14=O18	123.48	123.55	
C14-C15-H16	108.58	108.56	109
C14-C15-H17	113.56	113.67	112
C14-C15-H19	108.52	108.49	109
H16-C15-H17	109.42	109.41	109
H16-C15-H19	107.54	107.47	107
H17-C15-H19	109.02	109.03	109

Conformational Analysis

The optimized geometry of the acetazolamide is obtained using B3LYP/6-311++ G (d, p) and used for conformational analysis of the molecule. Conformational analysis is performed by potential energy surface scan function using semi-empirical method PM6, varying the dihedral angle C1-N6-C14-C15 in the steps of 10° over one complete rotation 0-360°. The semi empirical method is recommended [36] for the conformational analysis, as it does the job faster than the density functional theory (DFT) methods with reliable results. The graphical result, total energy verses scan coordinates, of this conformer analysis is presented in Fig. 2. The graph clearly shows that there is only one minimum energy conformer which is the most stable conformer of the compound at 180° with energy value -68.568 Kcal/Mol. There are two conformers at 100⁰ and 260⁰ with energy -53.664 Kcal/Mol, which correspond to the maximum energy or the most unstable conformers of the compound. The conformers at 0⁰ and 360⁰ belong to the same configuration with energy -61.042 Kcal/Mol, which represent a *meta* stable configuration of the compound. The structure of the molecules at these *meta* and most stable conformations are shown in Fig. 2. The most stable conformer or structure of the compound has been used for all further computational analysis in this study. The Fig. 2a shows the different conformation of the title compound Acetazolamide.
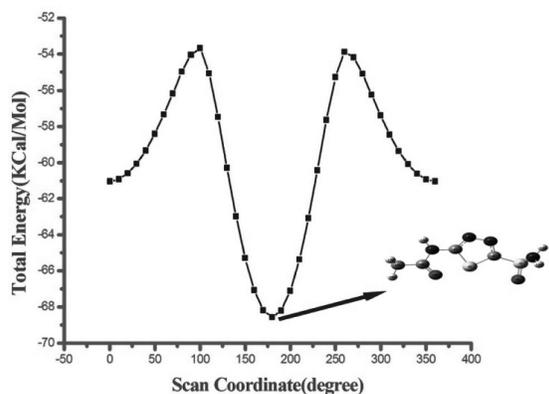
Fig. 2: Potential Energy profile of Acetazolamide
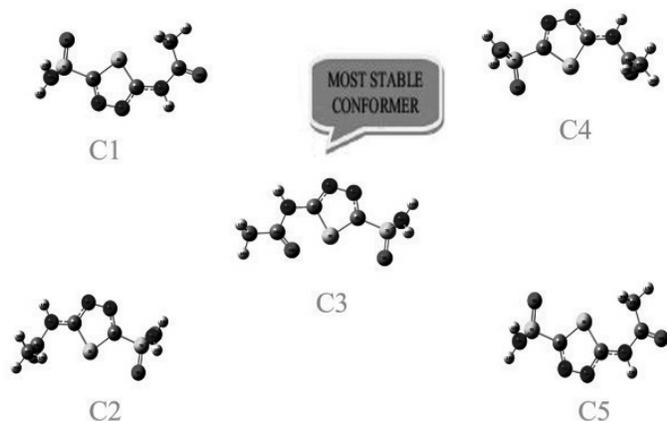
Fig. 2a: The different conformation of Acetazolamide

Fig. 3: Computational & Experimental FT-IR Spectrum of Acetazolamide

Vibrational Assignments

The title molecule acetazolamide has 19 atoms and it belongs to C_1 point group symmetry. The maximum number of potentially active observable fundamentals of non-linear molecule which contains N atom is equal to (3N-6), apart from three translational and three rotational degrees of freedoms. Hence the title molecule has 51 possible modes of vibrations. The 51 normal vibrations are distributed as

$$\tau_{vib} = 36\,A_g + 15\,A_u$$

The observed and calculated wave numbers using B3LYP and B3PW91 functional with the 6-311++G (d, p) basis set along with vibrational assignments are presented in Table 2. The assignments are carried out using the potential energy distribution (PED) values and also in comparison with literatures and with Gauss view software [27].   The experimental and calculated spectrum for the title molecule is presented in Fig. 3 and Fig. 4.

Fig. 4: Computational & Experimental FT-Raman Spectrum of Acetazolamide

C-H Vibrations

For all the aromatic compounds the carbon-hydrogen stretching vibrations are observed in the region 3100–3000 cm^{-1} and in aliphatic compounds in the region 3000–2900 cm^{-1} [37]. In the present molecule, there are only three C-H bonds in the methyl group in the acetamido part of the molecule. The observed values of these bands are at 3012, 3000 and 2910 cm^{-1}, which indicate all of them are aliphatic C-H bands but they are slightly higher than the usual value, this may be due to the absence of any aromatic C-H modes in this molecule.

The C–H in-plane bending and C-H out-of-plane bending vibrations are normally found in the range 1000–1300 cm^{-1} and 750–1000 cm^{-1}, respectively; with aromatic compounds occupying the higher side and aliphatic compound in the lower side of the range respectively [38, 39]. In the present case, the in-plane bending modes are observed at 1434, 1365 and 1087 cm^{-1} and the out-of plane bending are observed at 452, 413, 401 cm^{-1}. The in-plane bending vibrations lies in the expected range except first vibration and out-of plane bending vibrations are almost completely below the expected range, which indicate the presence of C-N, C-S, N-H have heavily influenced the C-H bending modes. The total energy distribution (TED) values confirms these interactions, they all lie as mixed modes in these region. The observation of calculated wave numbers using B3LYP and B3PW91 methods with the 6-311++G (d, p) basis shows good agreement between the methods as well as experimental values.

C-C, C=N, C-N Vibrations

In the aromatic compound, the C-C stretching vibrations are observed in the range of 1430-1650 cm^{-1}, with no clear cut demarcation between single and double bond within the ring, the C-C in aliphatic compounds will spread slightly above and below this range, C=C have values above 1600 cm^{-1} and C-C values below 1400 cm^{-1} [40-42]. In the present case, there is only one C-C bond in the acetamido group. The stretching vibration of this bond is observed at 1286 cm^{-1}. The in plane and out-of plane bending vibrations are observed at 701 and 270 cm^{-1}. All the vibrations are almost at the same expected places; hence, the C-C modes may be independent of other modes in the molecule. The total energy distribution (TED) values for these modes also

support this observation; the percentage contributions are relatively high for these C-C modes when compared to other modes which appear mixed with these modes.

The identification of C-N vibrations is a very difficult task, since mixing of several bands are possible in this region. Silverstein et al. [43] assigned C-N stretching absorption for aromatic amines in the region 1382–1266 cm^{-1}. In benzamide the band observed at 1368 cm^{-1} is assigned to be due to C-N stretching [44]. In benzotrizole, the CN stretching is found to be present at 1382 and 1307 cm^{-1}. In the present work, There are two C=N bonds and two C-N bonds, hence, the two bands observed at 1465, 1420 cm^{-1} and 1261 1176 cm^{-1} are assigned to C=N and C-N stretchings respectively. These values are though very well within the expected range, they do not exactly coincide with the values observed in molecules like 2, 6 diamino purine, 5, 6-dimethyl benzimidazole and 4-hydroxyquinone etc which confirms that these modes are very delicate and easily mix with other modes. The in-plane and out-of plane bending of C-N bonds are observed at 916, 621 and 155, and 125 cm^{-1} respectively. These bands are considerably below the normal range which indicates the interaction or influence of other modes in this range is very high. All these observations are supported TED distribution among the interacting modes by the relatively equal contributions of these modes.

N-H Vibrations

The hetro aromatic molecule containing an N-H group shows its stretching absorption in the region 3500-3200 cm^{-1}, which is usual range of appearance for N-H stretching [45, 46]. In this case, there are two N-H bonds in the sulphonamide group and one N-H in acetamido group; hence the top three frequencies observed in the IR at 3539, 3450 and 3301 cm^{-1} in this range are assigned to N-H stretching modes. The respective in-plane bending modes are observed at 1634, 1606, 1476 cm^{-1} and that of out-of plane bending modes at 610, 555, and 511 cm^{-1}. In the case of benzohydraside, these vibrations are found at 3250 1165 and 890 cm^{-1} respectively. The comparison with this literature values and also the total energy distribution (TED) distributions clearly indicate these modes are very prominent modes; they remain almost uninfluenced by other modes. However, the in-plane and out of plane modes are slightly undermined by the other mixed modes particularly the C-N and N-N modes.

S=O, C-S and S-N Vibrations

According to the literature, the SO stretching is observed at 1345 & 1347 cm^{-1} [7] and 1171 cm^{-1} [8]. The in-plane and out of plane bending are observed at 580 and 360 cm^{-1}[47] respectively. In this molecule, there are two S=O bonds, hence, there should be two stretching, two in-plane bending and two out-of plane bending vibrations; which are observed in this case at 1321 and 1130 cm^{-1}, 600 and 465 cm^{-1}, and 283 and 198 cm^{-1} respectively. Only the stretching vibrations are found in the expected range and other two in-plane and the out-of plane modes are above the expected range, which may be due to the difference in conjugational effect or the distribution of electrons in the bonds surrounding the S atom, between the reference molecule and the present molecule. The C-S and S-N stretching in the present molecule are observed at 839, 817, 673 cm^{-1} and 1045 cm^{-1} respectively, whereas in the cited literature [47] these values are less, which may also be due to the delicate interaction of various modes in these ranges, as indicated by the total energy distribution (TED) distributions among the mixed modes.

Table 2: The observed FTIR, FT–Raman and calculated frequencies using B3LYP & B3PW91 method with basis set 6-311++G(d,ρ) of the molecule Acetazolamide

S. No.	Symmetry species	Observed frequency (cm^{-1})		Scaled frequency (cm^{-1})		Vibrational assignments	% TED Assignment
				B3 LYP	B3 PW91		
		FT-IR	FT-Raman	6-311++ G (d, p)			
1	A$_g$	3539vw		3583	3565	ν N-H	νNH(99)
2	A$_g$	3450vs		3559	3472	ν N-H	νNH(100)
3	A$_g$	3301m		3472	3390	ν N-H	νNH(99)
4	A$_g$	3012vs		3055	3017	ν C-H	νCH(99)
5	A$_g$		3000w	3079	3006	ν C-H	νCH(99)
6	A$_g$	2910m		2935	2931	ν C-H	νCH(100)
7	A$_g$	1678vs	1680m	1737	1703	ν C=O	νCO(82)
8	A$_g$		1634w	1609	1548	β N-H	βNH(89)
9	A$_g$		1606vw	1578	1529	β N-H	νCN(49) + βHNC(41)
10	A$_g$		1476vw	1472	1468	β N-H	βHNH(80) + δCHCH(11)
11	A$_g$		1465vw	1460	1459	ν C=N	νCN(84)
12	A$_g$	1434s		1452	1438	β C-H	βHCH(82) + δCHCH(12)
13	A$_g$		1420vs	1410	1414	ν C=N	ν CN(48) + βHNC(22)
14	A$_g$	1365vs		1387	1370	β C-H	βHCH(94)
15	A$_g$	1321vs		1323	1343	ν S=O	ν SO(90)
16	A$_g$	1286m		1297	1307	ν C-C	νCC(51) + βCN(11)
17	A$_g$		1261m	1234	1203	ν C-N	νCN(21) + νCC(14) +βHNC(17) + δCHCH(15)
18	A$_g$	1176vs	1170s	1162	1158	ν C-N	νCN(60)
19	A$_g$		1130s	1103	1122	ν S=O	νSO(61) + νNN(13)
20	A$_g$	1087m		1077	1071	β C-H	βCHN(74)

21	A_g	1045m		1045	1056	ν S-N	νSO(10) + νSC(18) + βNCS(43)
22	A_g	1026m		1042	1030	ν N-N	βHCH(12) + δCNNH(65) + δOCNC(16)
23	A_g	974m		1001	996	β C=O	νCC(16) + δCHCO(49)
24	A_g		916m	958	962	β C=N	νNC(29) + νCC(18) +BCNC(13)
25	A_g	839w		834	843	ν C-S	νCS(56) + δNHSH(19) + δSNOO(11)
26	A_g	817w		791	796	ν C-S	βCSN(61)
27	A_g		701vs	681	691	β C-C	νCC(12) + νSC(48) + βCCN(12)
28	A_g	673s		656	665	ν C-S	νSC(21) + βCSC(43)
29	A_g	621 s		631	633	β C-N	δ NNCS(48) + δ OCNC(25) + δCSCN(11)
30	A_g		610w	615	613	δ N-H	δHNCC(19) + δNNCS(25) + δ OCNC(40)
31	A_g		600vw	598	602	β S=O	νSN(18) + δNHSH(12) + δSNOO(20)
32	A_g	584m		593	593	β N-S	δCSCN(62)
33	A_u	574w		572	566	β C-S	βCSC(11) + βCCO(19) + δNHSH(25)
34	A_u	555vw		544	542	δ N-H	δHNCC(21) + δSNOO(31)
35	A_u	511m		532	528	δ N-H	δHNCC(42) + δNHSH(11)
36	A_u		465m	472	475	β S=O	νSN(13) + βOSO(51) + δCSCN(10)
37	A_u		452s	421	423	δ C-H	βCCO(10) + βSCS(13) + δCHNO(37)
38	A_u		413w	381	382	δ C-H	βCCO(13) + βOSO(18) + δSCHN(15)
39	A_u		401s	365	367	δ C-H	βCSN(22) + δCHSN(19)
40	A_u		327vw	351	352	δ C=O	β NCN(12) + βCCO(31)
41	A_u		283vw	314	316	δ S=O	βNCC(11) + βCSO(38) + δHNSO(10)
42	A_u		270s	249	251	δ C-C	νSC(17) + βCSN(18) + δCSCN(10)
43	A_u		198vw	242	244	δ S=O	νSO(24) + βCSN(13)
44	A_u		183m	188	188	δ N-S	βCNC(14) + βSCS(20) + δHNSO(38)
45	A_u		155vs	148	148	δ C-N	βCNC(16) + βCSO(21) + δHNSO(22)
46	A_u		125s	121	122	δ C-N	βCSN(14) + δCNCC(27) + δCSCS(34)
47	A_g		82s	89	90	δ C-S	δCNCS(68)
48	Ag		72s	88	87	β C = N-N	βNCN(18) + βCNC(18) + βSCS(38)

49	A$_u$		54s	60	61	β N-N-C	δCNCC(27) + δCSCS(36) + δCSCN(22)
50	A$_u$		33m	35	32	δ N-C-S	δNCSN(85)
51	A$_u$		25w	25	25	δ C-S-C	δHCSC(65)

Natural Bond Orbital Analysis

In order to investigate the intra and inter-molecular interactions, the different possible donor orbitals, acceptor orbitals, their occupancy levels and the respective stabilization energies required for the transitions of the title compound were computed by using second-order perturbation theory at B3LYP/6-311++G (d, p) level. For each natural bonding orbital donor [NBO(i)] and natural bonding orbital acceptor [NBO(j)], the stabilization energy $E^{(2)}$ associated with electron delocalization between donor and acceptor is estimated [48, 49] using the relation;

$$E^{(2)} = \Delta E_{ij} = q_1 \frac{F(i,j)^2}{z_j - z_i}$$

Where q_i is the donor orbital occupancy, ε_i, ε_j are diagonal elements (orbital energies) and F_{ij} is the off-diagonal NBO Fock matrix element. The results of this computation are presented in Table 3.

The larger the stablisation energy $E^{(2)}$ value, the more intensive is the interaction between donor and acceptor orbitals i.e., the more the electron donating tendency from the donor orbitals and more the electron accepting tendency of the acceptor orbitals, the greater is the extent of conjugation of the whole system. Thus, the highest $E^{(2)}$ values indicate the most probable electronic transitions in the molecule. In the present molecule acetazolamide, as there is no benzene ring,

there is not even one C-C to C-C π-π* transition among the top most probable transitions. Based on $E^{(2)}$ values, the first six most probable transitions in this molecule in the descending order of probability are; N6→ C14 – O18 (n -π* 52.32 Kcal mol⁻¹), N6→ C1 – N4 (n -π* 45.64 Kcal mol⁻¹), S3→ C1 – N4 (n -π* 32.06 Kcal mol⁻¹), S3→ C2 – N5 (n -π* 27.27 Kcal mol⁻¹), O18→ N6 - C14(n - π* 25.80 Kcal mol⁻¹) and O8→ S7 - O9(n - π* 21.44 Kcal mol⁻¹).

The careful analysis of these transitions shows that two of these transitions, the third and fourth, are from the thiadiazole ring, the rest of them from the substitutional groups. Similarly, only those transitions from the ring are π →π* transitions, the first two transitions, which are from acetamide group, are n →π* transitions and the fifth one which is also from the same group belongs to π → σ * transition and the last one which is from sulphonamide group belongs to σ → σ * transitions. These σ → π*, π → σ*, and n → π* transitions are not usually happening in other organic molecules, particularly in aromatic compounds which may be the reason for enhanced biological activity of the acetazolamide. Among these probable transitions, some of them will not be present in actual UV-Vis spectrum of the compound, which can be ascertained using their respective oscillator strength values and HOMO-LUMO contributions, which is discussed in the following section.

Table 3: Second order Perturbation theory of Fock matrix in NBO basis of Acetazolamide using B3LYP with 6-311++ g(d, ρ)

Donor	Type of Bond	Occupancy	Acceptor	Type of Bond	Occupancy	Energy E(2) Kcalmol⁻¹	Energy difference E(j)-E(i) a.u.	Polarized energy F(i,j) a.u.
C1-S3	n	1.9720	C2-S7	σ*	0.22683	5.16	0.81	0.061
	n		N6-H13	σ*	0.01789	2.88	1.06	0.049
C1-N4	n	1.9893	N6-C14	σ*	0.08144	2.13	1.31	0.048
	π	1.9867	C2-N5	π*	0.33829	14.7	0.32	0.065
C2-S3	n	1.9752	C1-N6	σ*	0.03738	6.65	1.10	0.077
C2-N5	π	1.9192	C1-N4	π*	0.38660	9.02	0.33	0.053
	π		S7-N10	σ*	0.23229	2.19	0.48	0.030
C2-S7	n	1.9667	N4-N5	σ*	0.01645	3.46	1.10	0.055

	n		S7-O8	σ*	0.15115	2.63	1.00	0.047
	n		S7-O9	σ*	0.14574	2.55	1.00	0.046
N4-N5	n	1.9743	C1-N6	σ*	0.03738	4.69	1.25	0.069
	n		C2-S7	σ*	0.22683	4.45	0.96	0.061
N6-H13	n	1.9783	C1-S3	σ*	0.07435	5.52	0.87	0.063
	n		C14-O18	σ*	0.01392	3.46	1.28	0.060
S7-O8	n	1.9860	S7-N10	σ*	0.23229	2.35	1.12	0.049
S7-O9	n	1.9867		σ*		2.14	1.12	0.046
S7-N10	n	1.9805	S7-O8	σ *	0.15115	2.45	1.08	0.048
	n		S7-O9	σ *	0.14574	2.53	1.07	0.048
C14-C15	n	1.9842	C1-N6	σ*	0.03738	3.84	1.08	0.058
C15-H16	n	1.9754	N6-C14	σ*	0.08144	2.34	0.93	0.042
	n		C14-O18	π *	0.25335	3.85	0.52	0.042
C15-H17	n	1.9879	C14-O18	σ*	0.01392	4.89	1.13	0.066
C15-H19	n	1.9712	C14-O18	π *	0.25335	5.45	0.52	0.051
S3	n	1.9827	C1-N4	σ*	0.02681	2.36	1.23	0.048
	σ		C2-N5	σ*	0.02954	2.69	1.26	0.052
	π	1.5846	C1-N4	π *	0.38660	32.1	0.24	0.078
	π		C2-N5	π *	0.33829	27.2	0.24	0.073
N4	n	1.9081	C1-S3	σ*	0.07435	14.3	0.57	0.081
	n		C1-N6	σ*	0.03738	2.85	0.81	0.043
	n		C2-N5	σ*	0.02954	5.14	0.96	0.064
N5	n	1.9007	C1-N4	σ*	0.02681	5.37	0.92	0.064
	n		C2-S3	σ*	0.09083	14.6	0.57	0.082
	n		C2-S7	σ*	0.22683	2.98	0.51	0.036
N6	n	1.6572	C1-N4	π *	0.38660	45.6	0.27	0.099
	n		C14-O18	π*	0.25335	52.3	0.29	0.113
O8	n	1.9827	S7-O9	σ *	0.14574	2.13	1.11	0.045
	π	1.8007	C2-S7	σ*	0.22683	14.4	0.42	0.070
	π		S7-N10	σ *	0.23229	18.7	0.42	0.080
	σ	1.7651	C2-S7	σ *	0.22683	5.89	0.41	0.044
	σ		S7-O9	σ*	0.14574	21.4	0.58	0.101
	σ		S7-N10	σ*	0.23229	7.04	0.41	0.048
O9	π	1.8164	C2-S7	σ *	0.22683	16.4	0.42	0.075
	π		S7-N10	σ*	0.23229	12.4	0.42	0.066
	σ	1.7876	C2-S7	σ*	0.22683	2.17	0.42	0.027
	σ		S7-O8	σ*	0.15115	20.1	0.59	0.099
	σ		S7-N10	σ*	0.23229	11.3	0.42	0.062
N10	n	1.9207	C2-S7	σ*	0.22683	4.18	0.48	0.041
	n		S7-O8	σ*	0.15115	4.06	0.65	0.046
O18	π	1.8495	C2-S3	σ*	0.09083	2.20	0.46	0.029
	π		N6-C14	σ*	0.08144	25.8	0.69	0.121
	π		C14-C15	σ*	0.05000	18.9	0.64	0.101

UV-Vis & FMO Analysis

The calculations of the most probable electronic transitions of acetazolamide are performed at B3LYP/6-311++G (d, p) level using the time dependent self consistent field (TD-SCF) approach, along with IEF-PCM model to find ethanol solvent effect. The calculated values of excitation energies (E), oscillator strength (*f*) and absorption wavelength (λ) and HOMO-LUMO contributions for the first five most probable transitions are presented in Table 4. The pictorial representations of the frontier molecular orbitals; the HOMO and LUMO of the compound are shown in Fig. 6, the corresponding energy levels, other parameters calculated from these values such as electronegativity, global hardness and softness are presented in Table 5.

According to the Table 4, the energy gap for the top five transitions at gas phase are 4.693, 4.871, 5.129, 5.591 and 5.769 eV, the absorption wavelengths are 264, 254, 241, 221 and 214 nm, and the respective oscillator strengths are 0.0003, 0.2958, 0.0034, 0.0046 and 0.0069. Oscillator strength is the indicator of the absorption coefficient or the intensity of the peak of a particular transition in the UV spectrum of the compound, which is calculated based on the occupancy levels of the donor and acceptor orbitals. Hence, the above oscillator values indicate that only the second transition peak will have the observable intensity in the UV-Visible spectrum and other four peaks will have negligible height when compared to the second one. According to natural bonding orbital (NBO) analysis the transition which make the above peak is N6 → C1 – N4 (n →π* 45.64 Kcal mol⁻¹).

Table 4: Experimental and theoretical electronic absorption wavelength of Acetazolamide using TD-SCF/B3LYP/6-311++G(d, ρ)

Experimental			Theoretical			Major Contribution	Assignment
			TD-SCF				
λ (nm)	E(eV)	*f*	λ (nm)	E(eV)	*f*		
Gas							
			264.18	4.6931	0.0003	H-1 → L (97%)	n→ π*
			254.70	4.8719	0.2958	H → L (96%)	n→ π*
			241.70	5.1296	0.0034	H-2 → L (78%)	π →π*
			221.73	5.5916	0.0046	H-5 → L (32%)	π →σ*
			214.91	5.7691	0.0069	H-4 → L (25%)	σ→σ*
Ethanol							
292.26		0.6191	260.78	4.7544	0.3367	H → L (97%)	n→ π*
			258.62	4.7941	0.0038	H-1 → L (91%)	n→ π*
			241.04	5.1438	0.0009	H-2 → L (84%)	π →π*
			218.09	5.6849	0.0027	H-5 → L (21%)	π →σ*
			214.43	5.7819	0.0101	H-5 → L (24%)	σ→σ*

Table 5: HOMO, LUMO, Kubo gap, global electronegativity, global hardness and softness, global Electrophilicity index of Acetazolamide

Parameters	Acetazolamide		
	Optimized state	Transition state by TD-SCF	
	B3LYP/ 6-311++ G (d, p)	Gas	Ethanol
E_{HOMO} (eV)	7.7265	7.5589	7.5341
E_{LUMO} (eV)	1.3139	2.1226	2.1615
$\Delta E_{HOMO-LUMO\,gap}$ (eV)	6.4126	5.4363	5.3726
Electronegativity (χ) (eV)	4.5202	4.8404	4.8478
Global hardness (η) (eV)	3.2063	2.7181	2.6863
Global softness (σ) (eV)	0.3118	0.3679	0.3722
Electrophilicity index (ω) (eV)	3.1862	4.3098	4.3742
Dipole moment (μ) (Debye)	5.5539	5.5539	9.7957

In the ethanol phase, where the experimental spectrum also was recorded, the energy gap, absorption wave lengths and the oscillator strengths for the top five electronic transitions are 4.754, 4.794, 5.143, 5.684 and 5.781 eV, 260, 258, 241, 218 and 214 nm, & 0.3367, 0.0038, 0.0009, 0.0027 and 0.0101 respectively. These oscillator strength indicate that only the first transition will have notable intensity in the spectrum and the last one will make a small bump, other transitions will not be visible in the spectrum. This prediction is projected visually in the theoretical spectrum shown in Fig. 5a. The Fig. 5b shows the experimental spectrum which shows only one peak at 292 nm. This indicates that the theoretical prediction about the intensity of the peak is true, whereas there is difference of 32 nm in the absorption wavelength which may be an error in the theoretical calculation. According to the NBO analysis, the transition which causes this UV absorption is N6→ C14 – O18 (n → π* 52.32 Kcal mol^{-1}) which can very well fall at the experimental wavelength 292 nm. The comparisons of the two phases indicate that the solvents can change not only the wavelength of absorption but also the type of transition which appear in the spectrum.
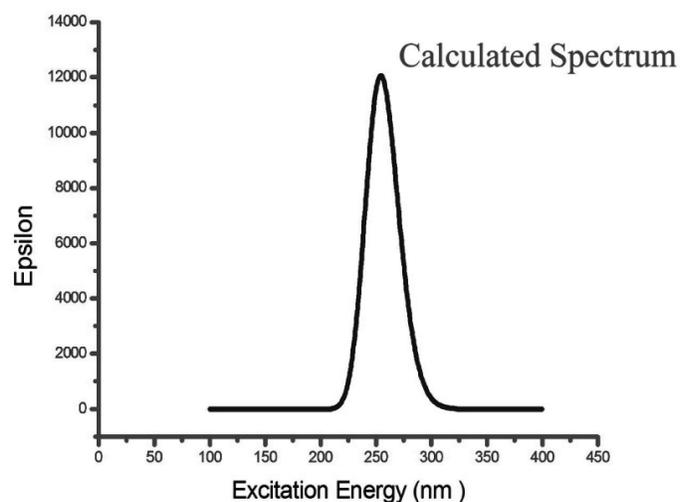
Fig. 5a: Calculated UV Spectrum of Acetazolamide
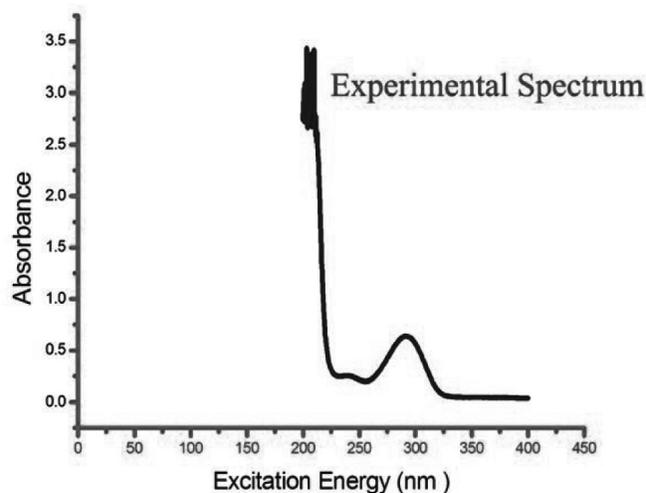
Fig. 5b: Experimental UV Spectrum of Acetazolamide
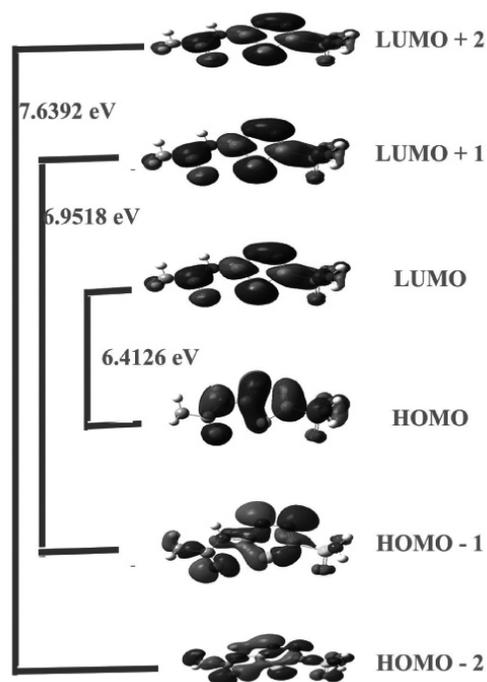
Fig. 6 Frontier Molecular Orbital of Acetazolamide

Table 6: Atomic Charges of Acetazolamide at B3LYP/6-311++ G (d, ρ)

Atom	B3LYP / 6-311 ++ G (d, p)	
	Mulliken Charge	APT Charge
1 C	-0.33807	0.72456
2 C	-0.40623	-0.07089
3 S	0.38706	0.13506
4 N	0.02305	-0.47505
5 N	-0.06677	-0.18598
6 N	-0.02104	-0.71263
7 S	0.44111	2.28396
8 O	-0.14027	-0.86434
9 O	-0.25258	-0.82485
10 N	-0.35222	-0.37698
11 H	0.30065	0
12 H	0.29532	0
13 H	0.31998	0
14 C	0.32392	1.12749
15 C	-0.73345	-0.01163
16 H	0.19443	0
17 H	0.13110	0
18 O	-0.30484	-0.74875
19 H	0.19885	0

Atomic Charge Analysis

The charge distribution on each atom of the molecule has an important influence on the NMR chemical shift and vibrational spectra. The atomic charges are computed by both Mulliken population analysis (MPA) and atomic polar tensor (APT) charge analysis methods using B3LYP functional with 6-311++ G (d, p) basis set and the values are tabulated in Table 6. The graphical presentation of the same for comparison purpose is shown in Fig. 7.

As can be seen in Fig. 7, among the four carbon atoms present in the molecule, C1 and C2 which are present inside the thia-diazole are found equally negative (-0.40623) in MPA, whereas C1 is highly positive (0.72456) while C2 is slightly negative (-0.07089) in APT. The prediction by APT is more probable as C1 is bonded to two N atoms but C2 is bonded to only one N atom, hence the loosing of electrons to N must be more in C1 than in C2, which makes the C1 more positive than C2.
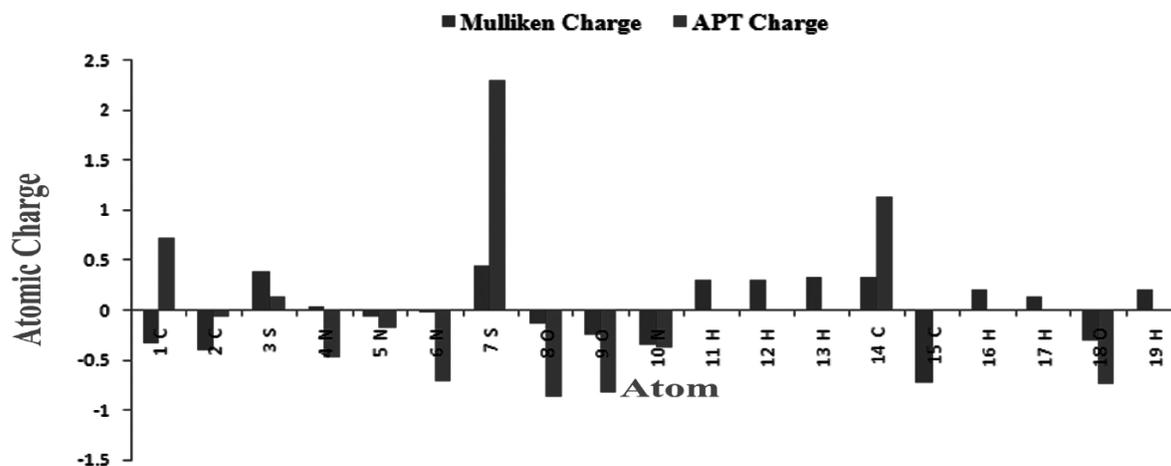
Fig. 7: Atomic Charge Analysis of Acetazolamide

Similarly, C15 carbon atom which is present in methyl group in acetamido part is highly negative (-0.73345) whereas C14 which is connected with C15 is positive (0.32392) in MPA, whereas in APT, the C15 is found to be almost neutral (-0.01163) while C14 is more positive than it is in MPA. C14 is bonded to N atom one side and O atom on other side along with C15, hence it may donate electrons to N and O as they have more electron attracting power than C, at the same time it can share the electrons with C15, as both of them have same electronegativity. Thus, prediction by APT that C14 is more positive while C15 is almost neutral seems more reasonable. However, the usual negative charge of methyl carbon atom has been assigned to C15 in MPA, which is proved to be correct in NMR chemical shift analysis.

Among the Nitrogen atoms, all the nitrogen atoms are predicted to be negative in APT, only the magnitude is different for all these atoms. N4 and N6 are relatively highly negative (-0.47505 and -0.71263), and N5 is the least negative (-0.18598) among them. In the case of MPA, N4 is slightly positive (0.02305), N5 is slightly negative (-0.06677) whereas N6 is almost neutral (-0.02104) and N10 is highly negative (-0.35222). This prediction by MPA is a surprising result as N atoms cannot be made positive unless it bonded with atoms which have more electron withdrawing power than N, like O etc. Among the two Nitrogen atoms within the thio diazole ring N4 & N5, N4 can be more negative than N5 as it can share electrons from N6 also, which is not possible for N5, but N4 cannot be made positive in this circumstances as predicted by MPA. The two sulphur atoms S3 and S7 are found to be equally positive (0.38706) in MPA, but S7 is extremely positive in APT while S3 is less positive. S7 is bonded with two O atoms on either side and with one N atom at the other side; hence there is more chance of losing all its electrons than S3 which is bonded only to two C atoms. Hence, the prediction by APT seems to be more reasonable in this case also. Among the hydrogen atoms, all the hydrogen atoms are predicted to be equally positive in MPA, irrespective of atom to which they are attached. But in APT the charges of all hydrogen atoms are found to be zero, which is not possible as they usually donate electrons to the atoms with which they are bonded.

Molecular Electrostatic Potential

The molecular electrostatic potential (MEP) surface is a method of mapping electrostatic potential of the rich and poor electron cloud in the molecule. The size and shape of the molecule and dipole moment of the molecule provide a visual method to understand the relative polarity. MEP map illustrates the charge distributions of molecules three dimensionally. The MEP of the molecule are computed by using B3LYP/6-311++G (d, p) method. MEP mapping is used to investigate the molecular structure with its physiochemical property relationships [50-53]. The MEP is often depicted using a color scheme such as red denoting the most negative, blue the most positive and other spectrum colors intermediate values [54-58].
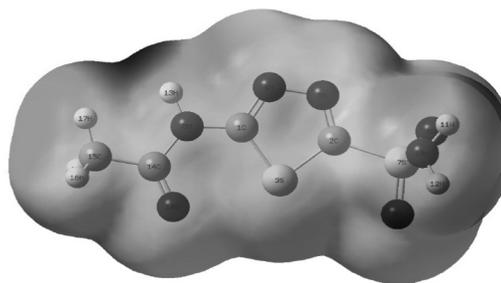
Fig. 8: MEP Map of Acetazolamide

The color code of the maps is in the range between -7.303 a.u. (deepest red) and 7.303 a.u (deepest blue) in compound. The red regions in the cloud are crowded around the negative nitrogen atoms and blue color is found among the hydrogen and some of the carbon atoms. The positive regions of MEP related to electrophilic reactivity and the negative regions to nucleophilic reactivity shown in Figure 8.

NMR Spectral Analysis

Nuclear magnetic resonance (NMR) spectroscopy has proven to be an exceptional tool to elucidate information on the molecular structure and conformations. To provide an explicit assignment and analysis of ^{13}C and ^{1}H NMR spectra, theoretical chemical shift of the title compound are also computed through gauge independent atomic orbital theory (GIAO) and B3LYP)/6-311+G (2d, p) basis set [59], along

with IEF-PCM to find the DMSO solvent effect. The theoretical ^{13}C NMR and ^{1}H chemical shifts along with the experimental values are presented in Table 7 and the respective spectra are presented in Fig. 9 and Fig. 10 respectively.

Atom Position	Experi -mental Value	Gas TMS/ B3LYP/6-311+G (2d,p) GIAO (ppm)	Solvent-DMSO TMS/ B3LYP/6-11+G(2d,p) GIAO (ppm)
1C	161	168.29	170.21
2C	170	176.87	177.46
14C	164	170.12	174.84
15C	23	22.567	23.47
11H (Amino)	8.57	8.1607	8.7378
12H (Amino)	7.46	4.3221	4.8451
13H (Amino)	7	4.2379	4.6994
16H (Methyl)	6.32	2.3482	2.4191
17H (Methyl)	6.32	2.3482	2.4191
19H (Methyl)	4.50	1.7159	2.1355

The chemical shift for aromatic carbon atoms usually lies in the range 120- 130 ppm [39-41], Table 7 shows, none of the carbon atom in the present molecule possesses this value which means none of these carbon atom is aromatic. The two carbon atoms C1 and C2 in the thia diazole ring have chemical shift values 161 and 170 ppm experimentally, 168 and 178 ppm theoretically, respectively. This supports the charge prediction by APT method for these two atoms, where C1 is found to be more positive while C2 is almost neutral.

The C14 which is extremely positive in APT in the acetamido part has chemical shift 164 ppm experimentally and 170 ppm theoretically. This is also in tune with charge predicted by APT than MPA. All these values are relatively high compared to usual carbon atoms in benzene or in methyl group; the reason for this phenomenon is the presence of N and O atoms in the neighborhood of these atoms. Whereas the C15 which is in the methyl group has very small chemical shift 23 ppm experimentally and 22 ppm computationally. This is the usual chemical shift value for any methyl group carbon atom, which shows the chemical environment C15 is not much deviated as predicted by APT, whereas it is closer to the usual negative charge predicted by MPA.
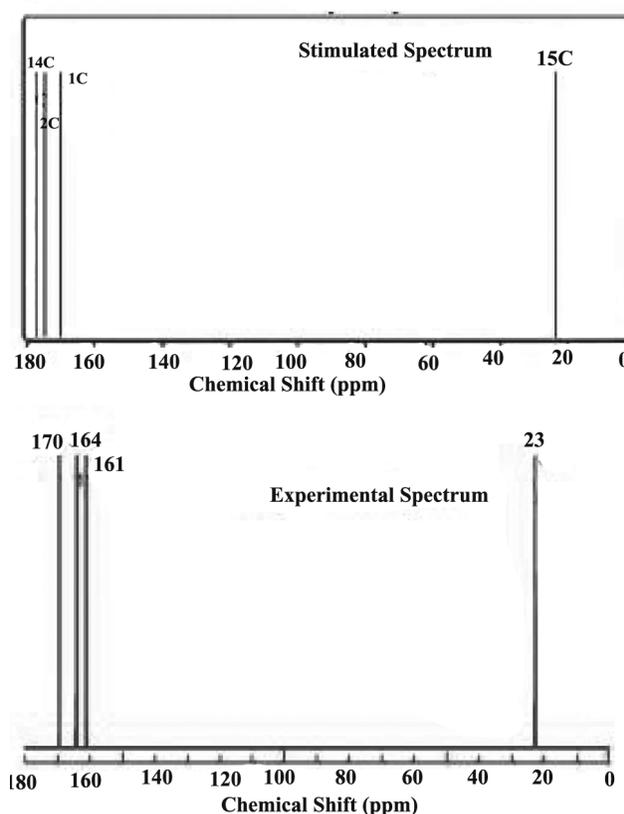
Fig. 9: ^{13}C NMR of Acetazolamide
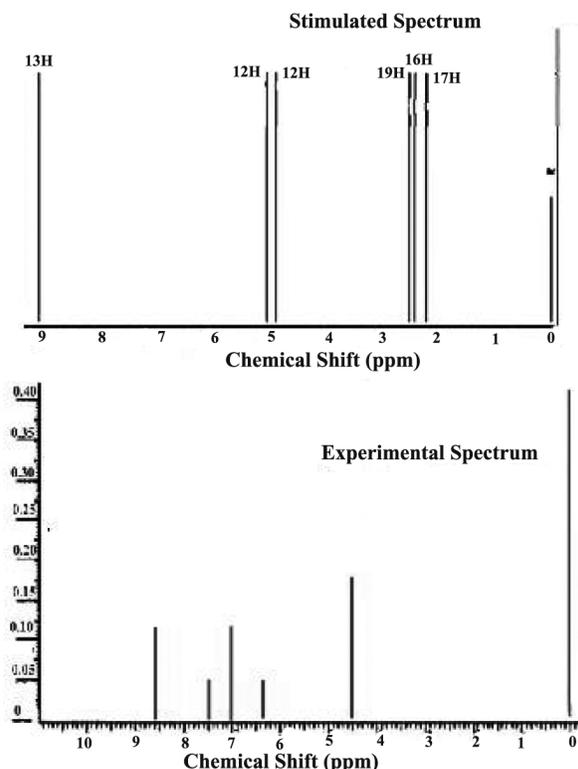
Fig. 10: ¹H NMR of Acetazolamide

In the case of Hydrogen atoms, the hydrogen atoms in the benzene ring generally have chemical shift values between 7 to 8 ppm, [60] but in this molecule all the hydrogen atoms except those of methyl group have almost same value between 6.3 to 8.5 ppm experimentally, between 4.2 to 8.1 ppm theoretically. This observation indicates that experimentally these hydrogen atoms have the same chemical atmosphere as the benzene hydrogen atoms with small deviation which is naturally due to the influence of N and O atoms in the molecule. Theoretically more deviations are shown but this is not proven to be correct experimentally. The methyl group hydrogen atoms have shown chemical shift around 2 ppm theoretically, which is the usual case but experimentally these values are found to be around 6 ppm. This is a surprising result as it is almost

close to benzene hydrogen atoms. In this case, the charge prediction by MPA (almost equally positive) is found to be more correct than that of APT.

Non Linear Optical Analysis

In order to investigate the relationships among molecular structures and non-linear optical properties (NLO), the dipole moment, polarizability and first hyperpolarizability of the acetazolamide compound were calculated by using B3LYP/6-311++ G (d, p). The polarizability (a_{ij}) and hyperpolarizability tensors (β_{ijk}) are obtained from Gaussian frequency output file. However, these values of the Gaussian output are in atomic units (a.u.), so they have been converted into electrostatic unit (esu) by using the relation, for a; 1 a.u. $= 0.1482 \times 10^{-24}$esu and for β; 1 a.u. $= 8.6393 \times 10^{-33}$esu. The hyperpolarizability and its components of acetazolamide along with related properties μ_0, α_{total} and $\Delta\alpha$ are reported in Table 8.

The calculated value of the dipole moment μ_0 is found to be 5.5539 Debye. The highest value of the dipole moment is observed for component μ_z, equal to 3.0358Debye and the lowest value of the dipole moment is along x direction μ_x and the value is -4.5184 Debye. The calculated average polarizability and anisotropy of the polarizability is -8.3954x10⁻²⁴esu and 13.4597x10⁻²⁴esu respectively. The hyperpolarizability is the important key factor which determines the non linear optical (NLO) activity of the molecule, which is normally compared with hyperpolarizability value of Urea, as it is used as the reference molecule for NLO activity. Hyperpolarizability value of the compound is 849.2949x10⁻³³esu. But the dipolemoment and hyperpolarizability of urea are 1.3732 D and 372.89 x10⁻³³esu respectively [35]. The comparison shows that the present molecule has both values higher than that of urea; hence the present molecule acetazolamide is a better NLO molecule.

Table 8: The Dipole moment (μ) (Debye), Polarizability (α) and hyperpolarizability (β) of Acetazolamide

Parameter	a.u.	×10⁻²⁴ e.s.u	Parameter	a.u.	×10⁻³³e.s.u
α_{xx}	-64.527	-9.5630	β_{xxx}	-79.537	-687.15
α_{xy}	-8.4581	-1.2534	β_{xyy}	-0.57832	-4.9961
α_{yy}	-102.25	-15.154	β_{xzz}	7.8585	67.892
α_{xz}	13.324	1.9746	β_{yyy}	-6.3621	-54.964
α_{yz}	-0.35311	-0.05231	β_{yxx}	28.184	243.49
α_{zz}	-3.1663	-0.46923	β_{yzz}	-7.3508	-63.505
α_{tot}	-56.649	-8.3954	β_{zzz}	3.0110	26.013
$\Delta\alpha$	90.822	13.459	β_{yyz}	6.0077	51.902
μ_x (Debye)	-4.5184		β_{xxz}	56.046	484.20
μ_y (Debye)	1.1015		β_{tot}	98.306	849.29
μ_z (Debye)	3.0358				
μ_{tot} (Debye)	5.5539				

Thermodynamic Properties

The values of the thermodynamical parameters: standard heat capacities (C) standard entropies (S), and standard enthalpy (H) of the compound were computed for different temperature starting from 100 to 500 K using B3LYP/6-311++G(d, p) level. The data are tabulated in Table 9. It has been found that when the temperature increases, the population is also raised at the particular energy level, thereby the disorder occurs in the system, and as a result all other thermodynamical parameters increases corresponding to the rise and fall of the temperature [43, 44]. The data of the thermodynamical parameters of heat capacities, entropies, enthalpy corresponding to the changes of temperatures were fitted by quadratic formulas and the corresponding fitting factors (R^2) for these thermodynamic properties are 0.9979, 0.9988 and 0.9986 respectively.

The fitting equations are given below and the correlation representation of the graphs are shown in Fig.11.

$$C = 4.36033+0.04898T+9.451933.615\times10^{-5}T^2$$
$$(R^2 = 0.9979) \ (SD=0.14228)$$
$$S = 47.5944+0.14144T-9.10509 \times 10^{-5}T^2$$
$$(R^2 = 0.9988) \ (SD=0.4429)$$
$$H = 84.325+0.00149T+4.22395\times10^{-5}T^2$$
$$(R^2 = 0.9986) \ (SD=0.02324)$$

Table 9: Thermodynamic properties at different temperatures at the B3LYP/6-311++G (d, p) level of Acetazolamide

T (K)	Heat capacity (cal mol⁻¹ K⁻¹)	Entropy (cal mol⁻¹ K⁻¹)	Enthalpy (Kcal mol⁻¹)
100	18.019	73.458	76.674
200	31.774	91.583	79.170
300	44.113	107.67	82.980
400	54.248	122.37	87.918
500	62.110	135.81	93.754
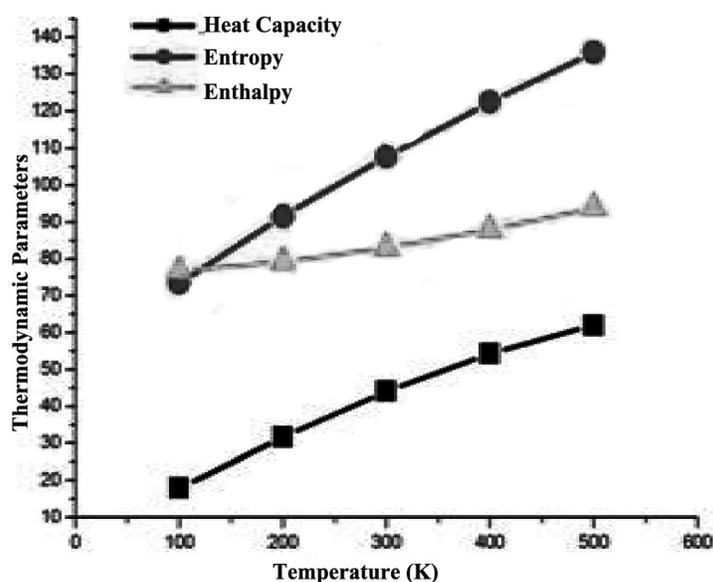
Fig. 11 Thermodynamic parametric variation with temperature of Acetazolamide

All the thermodynamic data will supply helpful information for the further study on the Acetazolamide which can be used to compute the other thermodynamic function using the standard equations and estimate chemical reactions.

CONCLUSION

The compound Acetazolamide has been subjected to systematic spectral analysis using the experimental FTIR, FT-Raman, 13C-NMR and 1H-NMR spectra, under the background of DFT computations supported by suitable basis sets. The structural analysis showed that the C-S bond lengths are shortened in thiadiazole ring formation whereas it remains unaffected outside. The minimum energy conformer which is the most stable conformer of the compound was obtained at 180° with energy value -68.568 Kcal/Mol. According to the NBO analysis, the transition which causes the UV absorption in the molecule is N6 → C14 – O18 (n → π* 52.32 Kcal mol^{-1}) which falls at wavelength 292 nm experimentally. The comparison of the gas and ethanol phases indicates that the solvents can change not only the wavelength of absorption but also the type of transition which appear in the spectrum. Among the atomic charges predicted by Mullikan and APT methods, the prediction by APT seems to be more reasonable when correlated with NMR chemical shift values. Hyperpolarizability value of the compound was found to be 849.2949×10^{-33} esu which shows that the present molecule acetazolamide will exhibit a better NLO activity. The vibrational analysis indicates that the presence of C-N, C-S, N-H heavily influences the C-H bending modes. Similarly the C-N and N-H bending modes have also been influenced by the other mixed modes such as C-H and C-S etc. These bands are considerably below the normal range which indicates the interaction or influence of other modes in this range is very high. These observations are confirmed by PED distributions among the interacting modes, by the relatively equal contributions of these modes.

ACKNOWLEDGEMENTS

REFERENCES

1. M. Mathew, G.J. Palenik, J. Chem. Soc., Perkin Trans. 2, (1974) 532-536.

2. IP. Kaur, R. Smitha, D. Aggarwal, M. Kapil, Int. J. Pharm. 248 (2002) 1-14.

3. S. Chakravarty, K.K. Kannan, J. Mol. Biol. 243(1994) 298-309.

4. S.C. Sweetman, Martindale: The Complete Drug Reference; 32nd edition, Pharmaceutical Press, London, UK, 1999**.**

5. N.A. Kasim, M. Whitehouse, C. Ramachandran, M. Bermejo H. Lennernas, A.S. Hussain, H.E. Junginger, S.A. Stavchansky, K.K. Midha, V.P. Shah, G.L. Amidon, Mol. Pharmaceutics 1 (2004) 85-96.

6. C.T. Supuran, J Enzyme Inhib Med Chem. 28(2) (2013**)** 229-230.

7. A.E. Ozel, Serda Kecel Gunduz, Sefa Celik, Sevim Akyuz, Journal of Spectroscopy 2013 1-13**,**

8. C. Baraldi, M.C. Gamberini, A. Tinti, F. Palazzoli, V. Ferioli, J. Mol. Struct. 918 (2009) 88-96.

9. B.A. Teicher, S.D. Liu, J.T. Liu, S.A. Holden, T.S. Herman, Anticancer Res. 13 (1993) 1549-1556.

10. C.T. Supuran, F. Briganti, S. Tilli, W.R. Chegwidden, A. Scozzafava, Bioorg. Med. Chem. 9 (2001) 703-714.

11. G. Pala, Farmaco, Edizione Scientifica, 11(1956) 395-403.

12. U.J. Griesser, A. Burger, K. Mereiter, J. Pharm Sci. 86 (1997) 352-358.

13. G.E. Cami, E.E. Chufan, J.C. Pedregosa, E.L. Varetti, J. Mol. Struct. 570 (2001**)** 119-127.

14. J.C. Pedregosa, G. Alzuet, J. Borras, S. Fustero, S. Garcia-Granda, M.R. Diaz, Acta Cryst. C49 (1993) 630-633.

15. S. Ferrer, J. Borras, C. Miratvilles, A. Fuertes, Inorg. Chem., 29 (1990) 206-210.

16. S. Ferrer, J. Borras, C. Miratvilles, A. Fuertes, Inorg. Chem. 28 (1989**)** 160-163.

17. J.C. Pedregosa, J. Casanova, G. Alzuet, J. Borras, S. Garcia-Granda, M.R. Diaz, A. Gutierrez-Rodriguez, Inorg. Chim. Acta. 232 (1995**)** 117-124. doi: 10.1016/0020-1693(94)04376-7

18. J.C. Pedregosa, J. Borras, S. Fustero, S. Garcia-Granda, M.R. Diaz, Acta Cryst. C52 (1996) 1849-1851.

19. E.E Chufan, J.C Pedregosa, J. Borras, Vibrational Spectroscopy 15 (1997) 191-199.

20. E.E. Chufan, J.C. Pedregosa, S. Ferrer, J. Borras, Vibrational Spectroscopy 20 (1999) 35-45.

21. G. Cami, J. Server-Carrio, S. Fustero, J.C. Pedregosa, Acta Cryst. C56 (2000**)** 209-210.

22. E.E. Chufan, S. Garcia-Granda, M.R. Diaz, J. Borras, J.C. Pedregosa, J. Coord. Chem. 54 (2001) 303-312.

23. U. Hartmann, H. Vahrenkamp, Inorg. Chem., 30 (1991) 4676-4677.

24. S.A. Brandan, E. Eroglu, A.E. Ledesma, O. Oltulu, O.B. Yalcınkaya, J. Mol. Struct. 993 (2011) 225-231.

25. D. Chaturvedi, V. Gupta, P. Tandon, A. Sharma, C. Baraldi, M.C. Gamberini, SpectrochimIca Acta A, 99 (2012) 150-159.

26. Gaussian 09 Program, Gaussian Inc., Wallingford CT, 2010.

27. M.J. Frisch, G.W. Trucks, H.B. Schlegel, G.E. Scuseria, M.A. Robb, J.R. Cheeseman, J.A. Montgomery Jr., T. Vreven, K.N. Kudin, J.C. Burant, J.M. Millam, S.S. Iyengar, J. Tomasi, V. Barone, B. Mennucci, M. Cossi, G. Scalmani, N. Rega, G.A. Petersson, H. Nakatsuji, M. Hada, M. Ehara, K. Toyota, R. Fukuda, J. Hasegawa, M. Ishida, T. Nakajima, Y. Honda, O. Kitao, H. Nakai, M. Klene, X. Li, J.E. Knox, H.P. Hratchian, J.B. Cross, C. Adamo, J. Jaramillo, R. Gomperts, R.E. Stratmann, O. Yazyev, A.J. Austin, R. Cammi, C. Pomelli, J.W. Ochterski, P.Y. Ayala, K. Morokuma, A. Voth, P. Salvador, J.J. Dannenberg, V.G. Zakrzewski, S. Dapprich, A.D. Daniels, M.C. Strain, O. Farkas, D.K. Malick, A.D. Rabuck, K. Raghavachari, J.B. Foresman, J.V. Ortiz, Q. Cui, A.G. Baboul, S. Clifford, J. Cioslowski, B.B. Stefanov, G. Liu, A. Liashenko, P. Piskorz, I. Komaromi, R.L. Martin, D.J. Fox, T. Keith, M.A. Al-Laham, C.Y. Peng, A. Nanayakkara, M. Challacombe, P.M.W. Gill, B. Johnson, W. Chen, M.W. Wong, C. Gonzalez, J.A. Pople, Gaussian Inc., Wallingford, CT, (2004).

28. Yosuf Sert, Cagri Cirak, Fatih Ucan, Spectrochimica Acta A 107 (2013) 248-255.

29. Hakan Arslan, Ozetekin Agul, Spectrochimica Acta A 70 (2008) 109-116.

30. M.H. Jamroz, Vibrational Energy Distribution Analysis VEDA 4, Warsaw, 2004.

31. M.H. Jamroz, Spectrochimica Acta A 114 (2013) 220 - 230.

32. E. Cances, B. Mennucci, J. Tomasi, J. Chem. Phys. 107 (1997) 3032- 3041.

33. B. Mennucci, J. Tomasi, J. Chem. Phys. 106 (1997) 5151- 5158.

34. K. Wolinski, J.F. Hinton, P. Pulay, J. Am. Chem. Soc. 112 (1990) 8251 - 8260.

35. Yu-Xi.Sun, Qing-Li.Hao, Wen-Xian Wei, Zong-Xue Yu, Lu-De Lu, Xin Wang, J. Mol. Struct. (Theochem) 904 (2009) 74-82.

36. James J.P. Stewart, J.Mol. Model 13 (2007) 1173-1213.

37. G. Varasanyi, Assignments of Vibrational Spectra of 700 Benzene Derivatives, Wiley, New York, 1974.

38. M. Karaback, M. Cinar, M. Kurt, J. Mol. Struct. 885 (2008) 28-35.

39. D. Bakkiyaraj, S. Periandy, S. Xavier, J. Mol. Struc. 1108 (2016) 33-45.

40. George Socrates. Infrared and Raman Characteristics group frequencies third edition, wiley, New York, 2001.

41. D.N. Sathyanarayana, Vibrational Spectroscopy Theory and Application; New Age International Publishers, New Delhi, 2004.

42. V.R. Dani, Organic Spectroscopy; Tata-MacGraw Hill Publishing Company: New Delhi, (1995) 139–140.

43. M. Silverstein, G. Clayton Basseler, C. Morill, Spectrometric Identification of Organic Compounds, Wiley, New York, 1981.

44. R. Shanmugam, D. Sathyanarayana, Spectrochimica Acta A 40 (1984) 757-761.

45. V. Arjunan, S. Sakiladevi, T. Rani, C.V. Mythili, S. Mohan, Spectrochimica Acta A 88 (2012) 220-231.

46. G. Socrates, Infrared and Raman Charecteristic group frequencies, tables and charts; third edition Wiley, Chichester, 2001.

47. J. Baran Enrque, Juan Zinczuk, J. Raman Spectroscopy 37 (2006) 948-950.

48. D.W. Schwenke, D.G. Truhiar, J. Chem. Phys. 82 (1985) 2418-2427.

49. M. Gutowski, G. Chalasinski, J. Chem. Phys. 98 (1993) 4728-4738.

50. M. Srivastha, P. Rani, N.P.Singh, R.A. Yadav, Spectrochimica Acta A 120 (2014) 274-286.

51. L. Li, T. Cai, Z. Wang, Z. Zhou, Y.Geng, T. Sun, Spectrochimica Acta A 120 (2014) 106 – 118.

52. E. Lewars, Computational Chemistry- Introduction to the theory and applications of molecular Quantum Mechanics. Kluwer Academic Publishers, Norwell, MA. 2003.

53. J.B. Foresman, A.E. Frisch, Exploring Chemistry with Electronic Structure Methods, Secod ed., Gaussian, Pittsburgh, PA, 1996.

54. I. Fleming, Frontier Orbitals and Organic Chemical Reactions, John Wiley and Sons, New York, 1976.

55. J.S. Murray, K. Sen, Molecular Electrostatic Potentials, Concepts and Applications, Elsevier, Amsterdam, 1996.

56. J.M. Seminario, Recent Developments and Applications of Modern Density Functional Theory, vol. 4, Elsevier, 1996, pp 800-806.

57. T. Yesilkaynak, G. Binzet, F. Mehmet Emen, U. Florke, N. Kulcu, H. Arslan, Eur. J. Chem. 1 (2010) 1-5.

58. Ira N. Levine, Quantum Chemistry, seventh edition, PHI Learning Pri. Ltd. Delhi, 2013, pp. 461-462.

59. A.J.D. Melinda, Solid state NMR Spectroscopy; Principles and Applications, Cambridge Press, 2003.

60. S. Sebastian, N. Sundaraganesan, Spectrochimica Acta A 75 (2010) 941-952.